Robustness of topological insulating phase against vacancy, vacancy cluster, and grain boundary bulk defects

Xiaojuan Ni, Huaqing Huang, and Feng Liu [*]
Department of Materials Science and Engineering, University of Utah, Salt Lake City, Utah 84112, USA

(Received 3 January 2020; revised manuscript received 21 February 2020; accepted 3 March 2020; published 19 March 2020)

One distinguished property of the topological insulator (TI) is its robust quantized edge conductance against edge defect. However, this robustness, underlined by the topological principle of bulk-boundary correspondence, is *conditioned* by assuming a perfect bulk. Here, we investigate the robustness of the TI phase against bulk defects, including vacancy (VA), vacancy cluster (VC), and grain boundary (GB), instead of edge defect. Based on a tight-binding model analysis, we show that a two-dimensional (2D) TI phase, as characterized by a nonzero spin Bott index, will vanish beyond a critical VA concentration ($n_{\mathrm{v}}^{\mathrm{c}}$). Generally, $n_{\mathrm{v}}^{\mathrm{c}}$ decreases monotonically with the decreasing topological gap induced by spin-orbit coupling. Interestingly, the $n_{\mathrm{v}}^{\mathrm{c}}$ to destroy the topological order, namely, the robustness of the TI phase, is shown to be increased by the presence of VCs but decreased by GBs. As a specific example of a large-gap 2D TI, we further show that the surface-supported monolayer Bi can sustain a nontrivial topology up to $n_{\mathrm{v}}^{\mathrm{c}} \sim 17\%$, based on a density-functional theory–Wannier-function calculation. Our findings should provide useful guidance for future experimental studies of effects of defects on TIs.

DOI: 10.1103/PhysRevB.101.125114

Topologically protected edge states in a two-dimensional (2D) topological insulator (TI) are immune to nonmagnetic defects/impurities on the edge. This distinguished feature of TI is rooted in the fundamental principle of bulk-boundary correspondence of topology [1,2]. However, this compelling principle is *conditioned* based on the assumption of a perfect bulk without defects. In real materials, bulk defects occur ubiquitously, which if abundant enough will inevitably destroy the bulk topology and hence mitigate the robustness of topological edge states. Therefore, an intriguing and important question is how robust a TI phase can be against bulk defects. While the bulk defects have been studied in arsenene [3–5], antimonene [4,6], bismuthene [7–9], and three-dimensional (3D) bichalcogenide [10–13], their influence on topological properties, especially how different bulk defects would destroy topological order, have still not been studied sufficiently [6,7,14]. In this work, we attempt to address this outstanding question for the most typical defects of vacancy (VA), vacancy cluster (VC), and grain boundary (GB), first in general within the theoretical framework of the tight-binding (TB) model of 2D TI [15–18], and then specifically for a prototypical large-gap 2D TI, SiC-supported monolayer Bi, based on first-principles calculation.

Due to its large spin-orbit coupling (SOC) strength, both the bulk-truncated Bi(111) bilayer [19–22] and the hypothetically hydrogenated hexagonal bismuthene [17,23] have been theoretically predicted to be large-gap 2D TIs with a gap of ∼0.5 and ∼0.8 eV, respectively. Furthermore, based on a substrate-orbital-filtering mechanism acting like the hydrogenation effect [17], epitaxial films of bismuthene and monolayer of other group-V elements have been theoretically proposed to be grown on semiconductor surfaces, such as Si [17,18], Ge [24], and SiC [25], to form large-gap surface-supported 2D TIs. One of these theoretical proposals [25], the bismuthene on SiC has already been successfully grown in experiments [26]; a large topological gap (∼0.8 eV in agreement with theory) has been observed by spectroscopic measurements and explained by the substrate-orbital-filtering mechanism [17]. The next experiment is expected to be transport measurement of the quantized edge conductance, while the main challenge lies presumably in sample quality/size because epitaxial growth is inherently a nonequilibrium process so that the bismuthene film usually contains defects, such as VAs, VCs, and GBs. Here, we will determine a theoretical upper limit of critical VA concentration ($n_{\mathrm{v}}^{\mathrm{c}}$) in the epi-Bi film for the existence of the TI phase to possibly guide future experimental efforts.

We first investigate the effect of bulk defects on the robustness of 2D TI within the theoretical frameworks of the TB model of a honeycomb lattice with p_x and p_y orbital bases, where the TI phase arises from the gap opening induced by any finite SOC at the Dirac point [17]. The nontrivial topology of a defect-containing lattice is determined by calculating the spin Bott index (B_{s}) in real space as developed recently by us [27,28], where a topological phase transition (TPT) is identified by a sudden jump of B_{s} from 1 to 0 along with the disappearance of the topological edge state. It is found that the robustness of the TI phase increases generally with the increasing topological energy gap ($E_{\mathrm{g,TI}}$) opened by SOC. Interestingly, the gap-closing effect induced by VAs is weakened

[*]Corresponding author: fliu@eng.utah.edu

by the presence of VCs, somewhat surprisingly, but enhanced with two typical GBs, somewhat as expected. For a TI with a large gap of ∼0.78 eV, the upper limit of n_v^c before the topological gap closes can reach up to ∼17%. This is further confirmed by a specific case study of Bi on SiC, using density functional theory (DFT) with maximally localized Wannier functions (MLWFs). We will also discuss the implications of our theoretical results in relation to experiments.

The TB model with p_x and p_y orbitals centered at the atomic sites in a honeycomb lattice shown in the Supplemental Material [29] (see also Refs. [30–37]) can effectively capture the main electronic and topological properties in hydrogenated, halogenated, and substrate-supported bismuthene [17,18,38–42]. The generic lattice-model Hamiltonian with the nearest-neighbor hopping and on-site SOC is expressed as

$$H = \sum_{i\alpha} \varepsilon_\alpha c_{i\alpha}^\dagger c_{i\alpha} + \sum_{\langle i\alpha, j\beta\rangle} t_{i\alpha,j\beta} c_{i\alpha}^\dagger c_{j\beta} + \lambda_{SO} \hat{L}\cdot\hat{\sigma}, \quad (1)$$

where $c_{i\alpha}^\dagger = (c_{i\alpha\uparrow}^\dagger, c_{i\alpha\downarrow}^\dagger)$ are electron creation operators on the α orbital at the ith site and ε_α is the on-site energy of the α orbital. $t_{i\alpha,j\beta}$ is the hopping integral expressed within the Slater-Koster scheme [43]. λ_{SO} is the strength of SOC. $\hat{L}$ is the angular momentum operator and $\hat{\sigma}$ is the Pauli matrices.

It is well known that this TB model gives ideally four typical bands: two Dirac bands bracketed by two flat bands [18]. The Dirac points at $K(K')$ and two band touching points at Γ will be gapped by SOC. All gaps are topologically nontrivial. Here, without losing generality, we choose the model parameters to fit the most salient features of the electronic bands of the DFT calculations for Bi on SiC [29], with $\varepsilon_{px} = 0$, $\varepsilon_{py} = 0$, $\lambda_{SO} = 0.39\,\text{eV}$, $V_{pp\sigma} = 1.87$, and $V_{pp\pi} = -0.80\,\text{eV}$. These are slightly different from those used to fit the energy levels at the K point [38] or the upper valence bands from DFT calculations [39], because our focus here is to have a more accurate bandwidth at the Γ and K points and SOC splitting at the K point, which will change predominantly with the introduction of VA as discussed below. The simplicity of our TB model eases the calculation of B_s and edge states in the presence of defects for large system sizes, while meantime representing faithfully the TPT induced by bulk defects.

The calculations of the eigenspectra, B_s, and edge state of a nonperiodic system were carried out using a 30 × 30 lattice. Note that B_s is numerically dependent on the lattice size, and the lattice size of 30 × 30 has been confirmed to achieve a converged B_s [29]. Vacancies were randomly generated among all lattice sites for each given n_v, and VCs were introduced additionally by randomly generating two or three VAs on the neighboring sites simultaneously at certain time steps. The VA size distribution for two scenarios clearly shows that the averaged cluster size in the system with VCs is larger than that with VA alone, which contains predominantly the mono-VAs [29]. Two typical symmetrical GBs in a honeycomb lattice with misorientation angles 21.8° (GBI) and 32.2° (GBII) [29,44–49] were constructed and a pair of GB dipoles were induced to resume periodic boundary condition (PBC) as needed.

First, using $\lambda_{SO} = 0.39\,\text{eV}$ as fitted for Bi on SiC, we calculated the eigenspectra versus the state index (in place of bands versus momentum for crystals) as a function of n_v. We employed PBC and the open boundary condition (OBC), respectively, to examine the topological gap-closing and edge-state vanishing process with the increasing n_v. The main results are shown in Fig. 1 for two typical values of $n_v = 10\%$ and 20% as the examples to represent VA-defected bulk of nontrivial and trivial phases, respectively, in comparison with the perfect bulk of the TI phase ($n_v = 0$).

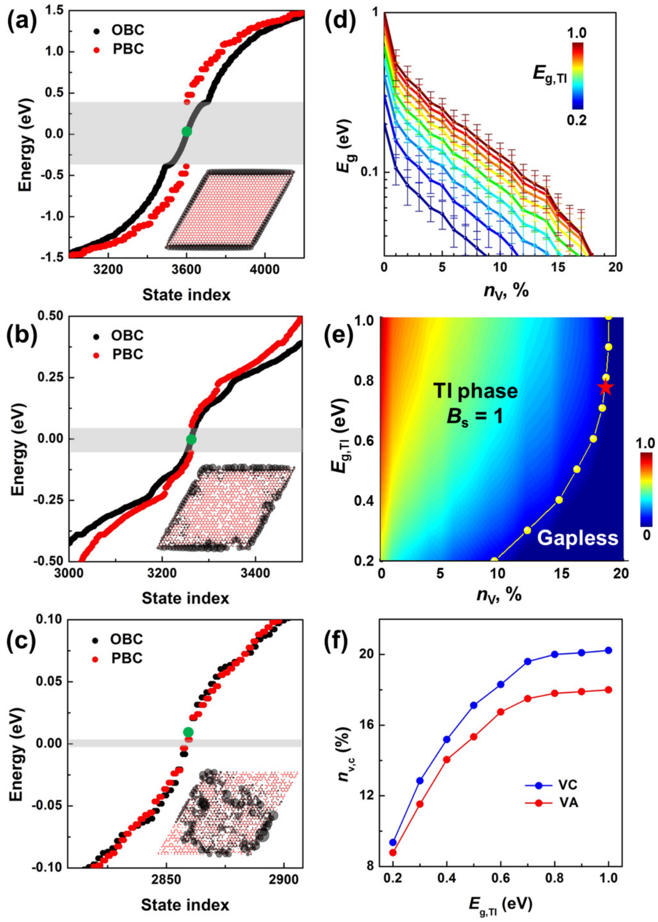

FIG. 1. Energy eigenvalues versus the state index obtained from the TB model in the presence of VA under PBC and OBC for (a) no VA, (b) $n_v = 10\%$, and (c) $n_v = 20\%$. The insets are the WFs of in-gap or near-gap states, marked by the green dots. The size of the black dot indicates the norm of the WF. (d) Semilog plots of energy gap versus n_v for different $E_{g,TI}$, from which $n_{v,c}$ is extracted at a gap size of 0.03 eV. (e) Phase diagram in the parameter space of $E_{g,TI}$ and n_v. The color indicates the energy-gap size under PBC. "Gapless" means the gap is effectively closed with a size smaller than 0.03 eV. The yellow line is the boundary between the TI phase and the gapless trivial phase. The red star represents the point of TPT for the Bi-on-SiC case. (f) The $n_{v,c}$ as a function of $E_{g,TI}$ in the presence of VA (red) and VC (blue).

Without VA, under PBC [red dots in Fig. 1(a)], the perfect bulk has an energy gap of ∼0.78 eV (twice of λ_{SO}) at half filling, in accordance with folding all the bands in K space into a single Γ point. Under OBC [black dots in Fig. 1(a)], some eigenvalues appear inside the original gap under PBC, implying that the system becomes "metallic." The inset in Fig. 1(a) shows the wave function (WF) of one of the in-gap states, marked by a green dot, which is completely localized on the edge. This indicates that the in-gap metallic state is characterized with a conducting edge, manifesting an insulating bulk and a conducting edge for a 2D TI. With the introduction of 10% VAs, under PBC [red dots in Fig. 1(b)], the energy gap is reduced to ∼0.12 eV. Under OBC, there appear some additional eigenvalues inside the gap [black dots in Fig 1(b)], which make the system become metallic, similar to the case of perfect bulk [Fig. 1(a)]. Also, the WF of one in-gap state, marked by a green dot, is shown in the inset of Fig. 1(b), which is localized on the edge. This indicates that the system with $n_v = 10\%$ remains a TI, having still an insulating bulk and a conducting edge, albeit with a smaller gap. In sharp contrast, further increasing n_v to 20%, under PBC [red dots in Fig. 1(c)], the bulk gap closes as one can no longer distinguish the in-gap states from the bulk states as the gap size is similar to the level spacings elsewhere. Then, under OBC [black dots in Fig. 1(c)], one can no longer identify an edge state. If one nevertheless picks one state next to the "gap" at half filling, marked by a green dot in Fig. 1(c), its WF shows no edge-related features [the inset in Fig. 1(c)]. Thus, an amount of 20% VAs has destroyed the TI phase and eliminated the topological edge states. We have also examined the eigenspectra and WFs of in-gap or near-"gap" states for other n_v, such as 13%–18% [29]. The n_v^c is extracted when the gap is smaller than 0.03 eV, and this empirical criterion is confirmed by the absence of the conducting edge state. From these calculations, we conclude that TPT from a TI phase to a trivial phase occurs at $n_v^c \sim 17\%$ [marked by the red star in Fig. 1(e) discussed below]. The B_s has been calculated to be indeed 1 for $n_v < 17\%$.

The above results suggest that the effect of VA to induce a TPT is triggered by a gap-closing mechanism. Then, one may expect the ability of n_v^c to close the gap is dependent on the topological gap, $E_{g,TI}$; namely, the larger the $E_{g,TI}$ is, the higher the n_v^c will be. To reveal this dependence, we have carried out a series of simulations to determine n_v^c as a function of $E_{g,TI}$. Figure 1(d) shows gap size as a function of n_v for different $E_{g,TI}$, from which n_v^c are extracted. Then, we construct a phase diagram in the parameter space of $E_{g,TI}$ and n_v, where the TI phase is characterized by a finite gap and $B_s = 1$ while the trivial phase is gapless, as shown in Fig. 1(e). For a typical range of $E_{g,TI} = 0.2 - 1.0\,\mathrm{eV}$, n_v^c increases from ∼9% to ∼18%.

Next, we include the effect of VCs in addition to VAs. Similar calculations are performed for $n_v = 14.8\%$ to 21.4% [29]. Surprisingly, n_v^c is larger with VCs for the same $E_{g,TI}$ than that with VAs, as shown in Fig. 1(f). For the same range of $E_{g,TI}$, n_v^c increases from ∼9% to ∼20% with VCs [29]. One way to understand this is that when VCs are introduced, the remaining regions are more "bulklike" with fewer VAs. One may consider the extreme scenario of all VAs coalesced into one big void; then the rest of the system remains a perfect bulk. The system with one big void sustains the TI phase up to an equivalent $n_v \sim 26\%$ for $\lambda = 0.39\,\mathrm{eV}$ [29], which is much larger than 17% with VAs and 19% with VCs, respectively.

Lastly, the effect of VAs in the presence of GBs was studied. First, we investigated the effect of GBs alone, which is known to generally affect the properties of materials [50], but its influence on TI is less studied. With PBC, the bulk band structures of a superlattice with GBI and GBII are shown in Figs. 2(a) and 2(b) with gaps of ∼0.75 and ∼0.51 eV, respectively, which are smaller than that of the perfect bulk of 0.78 eV, owing to the presence of GB states. The localized nature of the GB states is illustrated in the lower panels of Figs. 2(a) and 2(b), by plotting the WFs of the GB states. The band structures with edge states connecting bulk edge states for finite ribbons are shown in Figs. 2(c) and 2(d), and the localized edge-state WFs are shown in the lower panels. These results indicate that the two typical GBs considered here do not affect the TI phase. This is further confirmed by the nonzero B_s for a large system (2244 atomic sites with GBI and 3015 sites with GBII [29]).

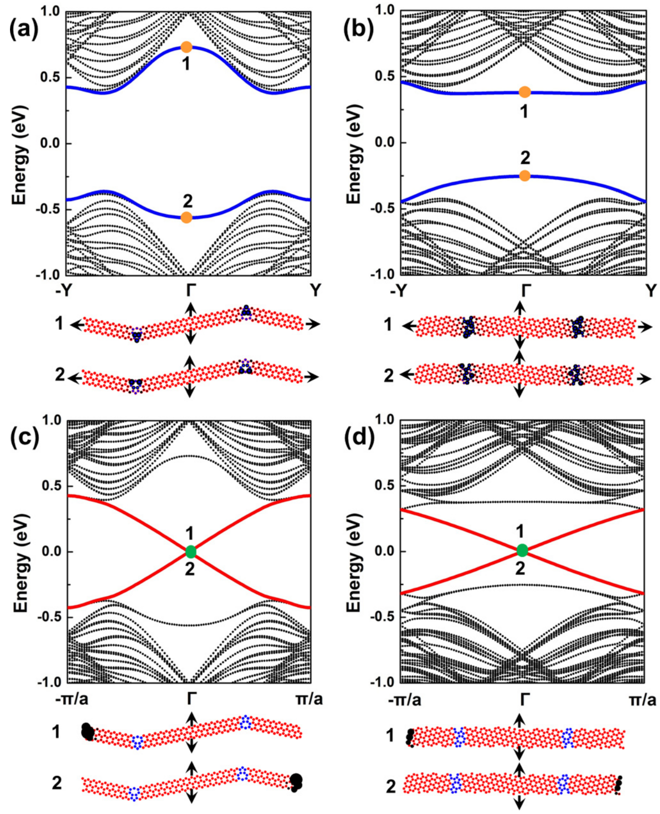

FIG. 2. (a),(b) The bulk band structures of a superlattice with GBI and GBII under PBC, respectively. Lower panels show the WFs of GBs states 1 and 2, marked by orange dots in the upper panels. (c),(d) Edge states of a finite ribbon with GBI and GBII, respectively. Lower panels show the WFs of edge states 1 and 2, marked by green dots in the upper panels. The atomic sites along the GBs are in blue. The size of the black dot indicates the norm of WF. The arrows indicate the periodic directions.

Next, we studied the effect of VAs in the presence of GBs. By introducing 5% VAs as examples, both systems with GBI and GBII maintain the TI phase, as characterized by the edge states in Figs. 3(a) and 3(b) and $B_s = 1$. The WFs for $n_v = 10\%$, 15%, and 20% are also calculated [29]. For a comparison, Fig. 3(c) shows the gap size decreasing with the increasing n_v for bulk, and bulk with GBs (I and II) in the presence of VAs. The n_v^c to close the gap are calculated to be ∼17%, ∼16%, and ∼15%, respectively. The in-gap states introduced by GBs essentially reduce the TI gap, which

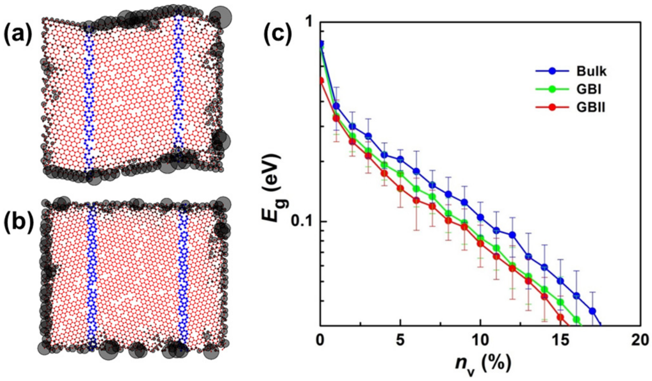

FIG. 3. (a),(b) The WFs of in-gap states for bulk with GBI and GBII at $n_v = 5\%$. The atomic sites along the GBs are in blue. The size of the black dot indicates the norm of the WF. (c) Semilog plots of energy gap versus n_v for perfect bulk (blue), bulk with GBI (green), and with GBII (red), from which the $n_{v,c}$ are extracted at a gap size of 0.03 eV.

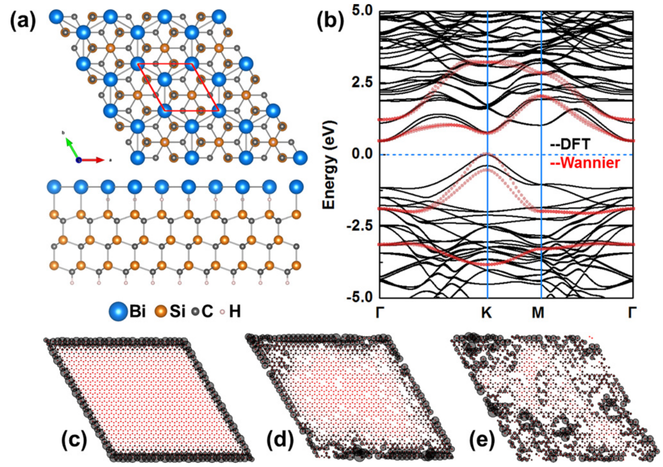

FIG. 4. (a) Top and side views of Bi-on-SiC structure. The red rhombus indicates the unit cell. The lattice constant is 5.36 Å. (b) First-principles (black) and Wannier (red) band structures. WFs of in-gap and near-gap states for (c) no VA, (d) $n_v = 10\%$, and (e) $n_v = 20\%$. The size of the black dot indicates the norm of the WF.

enhances the gap-closing effect induced by VAs. Therefore, in the presence of GBs, fewer vacancies can be tolerated in order to sustain the TI phase.

Beyond the TB analysis, we further demonstrate a material-specific calculation scheme to determine the robustness of topological order against VA formation in an experimentally synthesized large-gap 2D TI, Bi on SiC, based on the DFT-Wannier-function method. Figure 4(a) shows the top and side views of the Bi-on-SiC structure. The comparison of band structure between DFT and Wannier fitting is shown in Fig. 4(b). We note that the Wannier functions with p_x and p_y orbitals of Bi can well reproduce the band gap from DFT calculation, which is important for our analysis, but not the overall band dispersions (less important) due to the interference from the SiC-substrate electronic states. Using the Hamiltonian constructed from MLWFs, without VA, the in-gap WF shows well-localized edge states, as shown in Fig. 4(c). With the increasing of n_v, the edge states for $n_v = 10\%$ in the TI phase and 20% in the trivial phase are shown in Figs. 4(d) and 4(e), respectively. The edge states almost vanish at $n_v \sim 17\%$, which is confirmed by $B_s = 1$ for $n_v < 17\%$. These results agree well with those obtained above from the generic TB model. Here, we did not consider the structural relaxation of the defected systems since the surface-supported film can largely hold the bulk geometry in the presence of defects, and a recent study has shown that the TI phase can persist even in an amorphous state with local atomic displacements without "bulk" defects [51].

From an experimental point of view, epitaxial growth [52] of 2D TIs, such as Bi on SiC, is inherently a nonequilibrium process so that the thin film usually contains defects, such as VAs and GBs. The reported Bi-on-SiC film with a domain size of ~25 nm is believed to be considered as the limiting factor for transport measurements [26], as larger samples likely contain a higher concentration of VAs and GBs. Strikingly, our study suggests that the TI phase in Bi-on-SiC film with a large topological gap is not only immune to GBs, but also can sustain a rather high vacancy concentration up to about 15% without transitioning into a trivial phase. Therefore, it calls for a revisit of this system to look for larger samples below the critical defect concentration to facilitate transport measurements.

This work was supported by US Department of Energy-Basic Energy Sciences (Grant No. DE-FG02-04ER46148). We acknowledge the CHPC at the University of Utah and DOE-NERSC for providing the computing resources.

[1] B. A. Bernevig and T. L. Hughes, *Topological Insulators and Topological Superconductors* (Princeton University Press, Princeton, NJ, 2013).
[2] Z. F. Wang, K. Jin, and F. Liu, WIREs Comput. Mol. Sci. **7**, e1304 (2017).
[3] Y. Liu, Q. Zhou, W. Ju, J. Li, and Y. Liu, Superlattices Microstruct. **132**, 106163 (2019).
[4] X. Sun, Y. Liu, Z. Song, Y. Li, W. Wang, H. Lin, L. Wang, and Y. Li, J. Mater. Chem. C **5**, 4159 (2017).
[5] K. Iordanidou, J. Kioseoglou, V. V. Afanas'Ev, A. Stesmans, and M. Houssa, Phys. Chem. Chem. Phys. **19**, 9862 (2017).
[6] Z. Hu, J. Gao, S. Zhang, J. Zhao, W. Zhou, and H. Zeng, Phys. Rev. Mater. **3**, 074005 (2019).
[7] Y. Kadioglu, S. B. Kilic, S. Demirci, O. Ü. Aktürk, E. Aktürk, and S. Ciraci, Phys. Rev. B **96**, 245424 (2017).
[8] M. Qi, S. Dai, and P. Wu, Appl. Surf. Sci. **486**, 58 (2019).
[9] R. Gui, H. Jin, Y. Sun, X. Jiang, and Z. Sun, J. Mater. Chem. A **7**, 25712 (2019).
[10] D. Koumoulis, B. Leung, T. C. Chasapis, R. Taylor, D. King, M. G. Kanatzidis, and L. S. Bouchard, Adv. Funct. Mater. **24**, 1519 (2014).
[11] D. O. Scanlon, P. D. C. King, R. P. Singh, A. De La Torre, S. M. K. Walker, G. Balakrishnan, F. Baumberger, and C. R. A. Catlow, Adv. Mater. **24**, 2154 (2012).
[12] C. Niu, Y. Dai, Y. Zhu, Y. Ma, L. Yu, S. Han, and B. Huang, Sci. Rep. **2**, 976 (2012).

[13] S. Jia, H. Beidenkopf, I. Drozdov, M. K. Fuccillo, J. Seo, J. Xiong, N. P. Ong, A. Yazdani, and R. J. Cava, Phys. Rev. B **86**, 165119 (2012).
[14] S. T. Lee, S. M. Huang, and C. Y. Mou, J. Phys.: Condens. Matter **26**, 255502 (2014).
[15] C. L. Kane and E. J. Mele, Phys. Rev. Lett. **95**, 226801 (2005).
[16] C. L. Kane and E. J. Mele, Phys. Rev. Lett. **95**, 146802 (2005).
[17] M. Zhou, W. Ming, Z. Liu, Z. Wang, P. Li, and F. Liu, Proc. Natl. Acad. Sci. USA **111**, 14378 (2014).
[18] M. Zhou, W. Ming, Z. Liu, Z. Wang, Y. Yao, and F. Liu, Sci. Rep. **4**, 7102 (2014).
[19] S. Murakami, Phys. Rev. Lett. **97**, 236805 (2006).
[20] M. Wada, S. Murakami, F. Freimuth, and G. Bihlmayer, Phys. Rev. B **83**, 121310(R) (2011).
[21] Z. Liu, C. X. Liu, Y. S. Wu, W. H. Duan, F. Liu, and J. Wu, Phys. Rev. Lett. **107**, 136805 (2011).
[22] G. Bian, Z. Wang, X. X. Wang, C. Xu, S. Y. Xu, T. Miller, M. Z. Hasan, F. Liu, and T. C. Chiang, ACS Nano **10**, 3859 (2016).
[23] Z. Song, C. C. Liu, J. Yang, J. Han, M. Ye, B. Fu, Y. Yang, Q. Niu, J. Lu, and Y. Yao, NPG Asia Mater. **6**, e147 (2014).
[24] P. Li, M. Zhou, L. Zhang, Y. Guo, and F. Liu, Nanotechnology **27**, 095703 (2016).
[25] C. Hsu, Z. Huang, F. Chuang, C. Kuo, Y. Liu, and H. Lin, New J. Phys. **17**, 025005 (2015).
[26] F. Reis, G. Li, L. Dudy, M. Bauernfeind, S. Glass, W. Hanke, R. Thomale, J. Schafer, and R. Claessen, Science **357**, 287 (2017).
[27] H. Huang and F. Liu, Phys. Rev. B **98**, 125130 (2018).
[28] H. Huang and F. Liu, Phys. Rev. Lett. **121**, 126401 (2018).
[29] See Supplemental Material at http://link.aps.org/supplemental/10.1103/PhysRevB.101.125114 for supporting figures and discussion.
[30] G. Kresse and J. Furthmuller, Phys. Rev. B **54**, 11169 (1996).
[31] J. P. Perdew, K. Burke, and M. Ernzerhof, Phys. Rev. Lett. **77**, 3865 (1996).
[32] A. A. Mostofi, J. R. Yates, Y. Lee, I. Souza, D. Vanderbilt, and N. Marzari, Comput. Phys. Commun. **178**, 685 (2008).
[33] I. Souza, N. Marzari, and D. Vanderbilt, Phys. Rev. B **65**, 035109 (2002).
[34] N. Marzari and D. Vanderbilt, Phys. Rev. B **56**, 12847 (1997).
[35] J. Hoshen and R. Kopelman, Phys. Rev. B **14**, 3438 (1976).
[36] X. Ni, C. Hui, N. Su, W. Jiang, and F. Liu, Nanotechnology **29**, 075401 (2018).
[37] X. Ni, C. Hui, N. Su, R. Cutler, and F. Liu, Nanotechnology **30**, 185302 (2019).
[38] G. Li, W. Hanke, E. M. Hankiewicz, F. Reis, J. Schäfer, R. Claessen, C. Wu, and R. Thomale, Phys. Rev. B **98**, 165146 (2018).
[39] L. M. Canonico, T. G. Rappoport, and R. B. Muniz, Phys. Rev. Lett. **122**, 196601 (2019).
[40] G. F. Zhang, Y. Li, and C. Wu, Phys. Rev. B **90**, 075114 (2014).
[41] F. Dominguez, B. Scharf, G. Li, J. Schäfer, R. Claessen, W. Hanke, R. Thomale, and E. M. Hankiewicz, Phys. Rev. B **98**, 161407(R) (2018).
[42] Z. Liu, F. Liu, and Y. S. Wu, Chin. Phys. B **23**, 077308 (2014).
[43] J. C. Slater and G. F. Koster, Phys. Rev. **94**, 1498 (1954).
[44] A. Shekhawat, C. Ophus, and R. O. Ritchie, RSC Adv. **6**, 44489 (2016).
[45] O. V. Yazyev and S. G. Louie, Phys. Rev. B **81**, 195420 (2010).
[46] E. Annevelink, E. Ertekin, and H. T. Johnson, Acta Mater. **166**, 67 (2019).
[47] Y. Tison, J. Lagoute, V. Repain, C. Chacon, Y. Girard, F. Joucken, R. Sporken, F. Gargiulo, O. V. Yazyev, and S. Rousset, Nano Lett. **14**, 6382 (2014).
[48] Z. L. Li, Z. M. Li, H. Y. Cao, J. H. Yang, Q. Shu, Y. Y. Zhang, H. J. Xiang, and X. G. Gong, Nanoscale **6**, 4309 (2014).
[49] Y. Li, A. Wei, H. Ye, and H. Yao, Nanoscale **10**, 3497 (2018).
[50] I. A. Ovid'ko, in *Nanomaterials Handbook*, 2nd ed., edited by Y. Gugotski (CRC Press, Boca Raton, FL, 2017), pp.47–62.
[51] M. Costa, G. R. Schleder, M. Buongiorno Nardelli, C. Lewenkopf, and A. Fazzio, Nano Lett. **19**, 8941 (2019).
[52] J. W. Matthews, *Epitaxial Growth, Part 2*, rev. ed. (Elsevier, Amsterdam, 2017).